metals

MDPI

Review

Using Mini-CT Specimens for the Fracture Characterization of Ferritic Steels within the Ductile to Brittle Transition Range: A Review

Marcos Sánchez [1,*], Sergio Cicero [1,*], Mark Kirk [2], Eberhard Altstadt [3], William Server [4] and Masato Yamamoto [5]

[1] Laboratory of Materials Science and Engineering (LADICIM), University of Cantabria, E.T.S. de Ingenieros de Caminos, Canales y Puertos, Av./Los Castros 44, 39005 Santander, Spain
[2] Phoenix Engineering Associates, Inc., 119 Glidden Hill Road, Unity, NH 03743, USA
[3] Helmholtz-Zentrum Dresden–Rossendorf, Bautzner Landstrasse 400, 01328 Dresden, Germany
[4] ATI Consulting, Black Mountain, NC 28711, USA
[5] Central Research Institute of Electric Power Industry, Nagasaka 2-6-1, Yokosuka 240-0196, Japan
* Correspondence: sanchezmam@unican.es (M.S.); ciceros@unican.es (S.C.)

Abstract: The use of mini-CT specimens for the fracture characterization of structural steels is currently a topic of great interest from both scientific and technical points of view, mainly driven by the needs and requirements of the nuclear industry. In fact, the long-term operation of nuclear plants requires accurate characterization of the reactor pressure vessel materials and evaluation of the embrittlement caused by neutron irradiation without applying excessive conservatism. However, the amount of material placed inside the surveillance capsules used to characterize the resulting degradation is generally small. Consequently, in order to increase the reliability of fracture toughness measurements and reduce the volume of material needed for the tests, it is necessary to develop innovative characterization techniques, among which the use of mini-CT specimens stands out. In this context, this paper provides a review of the use of mini-CT specimens for the fracture characterization of ferritic steels, with particular emphasis on those used by the nuclear industry. The main results obtained so far, revealing the potential of this technique, together with the main scientific and technical issues will be thoroughly discussed. Recommendations for several key topics for future research are also provided.

Keywords: mini-CT; ductile-to-brittle transition range; reference temperature; master curve

Citation: Sánchez, M.; Cicero, S.; Kirk, M.; Altstadt, E.; Server, W.; Yamamoto, M. Using Mini-CT Specimens for the Fracture Characterization of Ferritic Steels within the Ductile to Brittle Transition Range: A Review. *Metals* **2023**, *13*, 176. https://doi.org/10.3390/met13010176

Academic Editors: Xiao-Wu Li and Peng Chen

Received: 22 December 2022
Revised: 10 January 2023
Accepted: 12 January 2023
Published: 15 January 2023

1. Introduction

Reactor pressure vessels (RPVs) are safety-critical components in nuclear power plants (NPPs). To ensure the continued operation of NPPs the fracture resistance of the RPV beltline materials is monitored throughout the plant's lifetime. RPVs are made of ferritic steels, which fail via a ductile mechanism at relatively high temperatures but transition to brittle fracture at lower temperatures. Additionally, the transition from ductile to brittle behavior is shifted towards higher temperatures when these steels are exposed to neutron irradiation. To ensure that ferritic steels maintain adequate structural integrity at service temperatures, actual RPV materials are included in surveillance programs that evaluate toughness behavior during their service life. These surveillance programs were originally based on impact energy measured from Charpy specimens. However, Charpy testing is used in a semi-empirical approach that cannot directly measure the material's fracture toughness. In the past several decades, a direct evaluation of the fracture behavior of RPV steels within the ductile to brittle transition range (DBTR) has been enabled by the master curve (MC) methodology, which has gained increased acceptance in recent years.

The MC is an engineering approach that provides a means to characterize the fracture behavior of ferritic steels within the DBTR [1,2]. The MC is standardized by ASTM E1921 [3]

and by JEAC4216 [4]. It is based on the weakest link theory and, thus, describes the fracture behavior using a three-parameter Weibull distribution. Two of the parameters, the location parameter (K_{min}) and the shape parameter (b), have been empirically defined for all ferritic steels (taking values of 20 MPa·$m^{0.5}$ and 4, respectively), whereas the scale parameter (K_0) has also been defined in terms of the material reference temperature (T_0). Thus, testing is performed to estimate this single material parameter. T_0 represents the temperature at which the median of fracture toughness, K_{Jcmed}, for a 1T (meaning 1-inch, or 25.4 mm) thick specimen is equal to 100 MPa·$m^{0.5}$. Once T_0 is estimated from K_{Jc} data for the material being analyzed, the MC can be defined for any probability of failure (P_f) by the following Equation (1):

$$K_{JC,\,Pf} = 20 + \left[\ln\left(\frac{1}{1-P_f}\right)\right]^{1/4} \cdot \{11 + 77 \cdot \exp[0.019 \cdot (T - T_0)]\} \quad (1)$$

In principle, T_0 can be defined by testing K_{Jc} specimens of any thickness. These test data are then scaled to a "1T-equivalent" K_{Jc} value, 1T". Thus, for miniature compact tension (mini-CT) specimens, the MC can be used to convert the measured K_{Jc} value into the corresponding $K_{Jc(1T)}$ equivalent, using the following equation (B being the thickness of the tested specimen, which is 4 mm for the mini-CT (2):

$$K_{JC(1T)} = 20 + [K_{JC} - 20]\left(\frac{B}{25.4}\right)^{1/4} \quad (2)$$

Hence, the MC addresses the three main characteristics of fracture toughness characterization within the DBTR: the scatter of the results, the dependency of fracture toughness on temperature, and the adjustment for test specimen thickness. Figure 1 shows an example of MC obtained by the authors in an ongoing program [5,6]. It is noted that the orange line defines a limiting condition in MC to consider the effect of the plastic zone evolution ahead of the crack tip, as discussed later in Section 2.5. All the K_{Jc} data above this line (red symbols) will be censored to account appropriately for their effect on T_0.

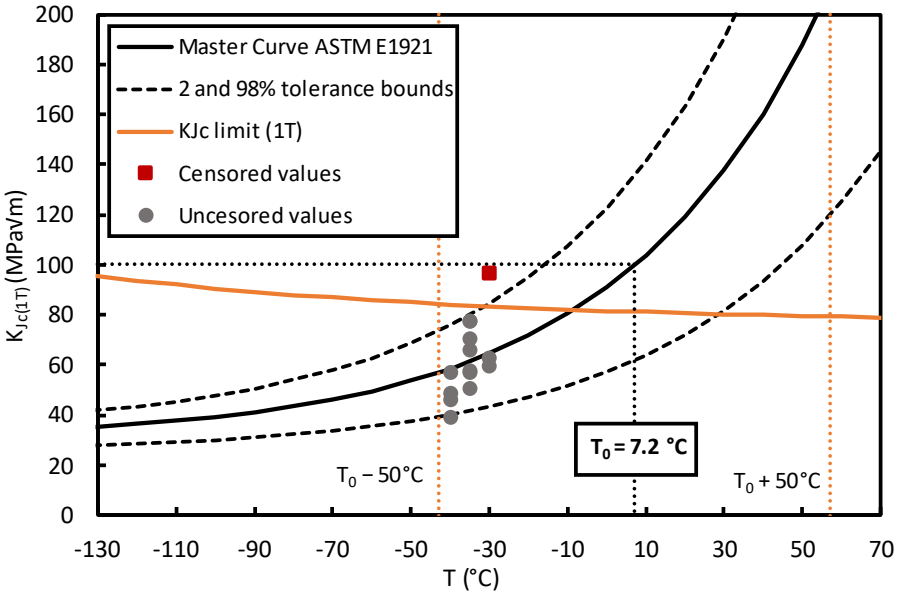

Figure 1. MC for A533B LUS, obtained using mini-CT specimens. Censoring criterion as defined by ASTM E1921 [3].

The need for accurate characterization of the DBTR faces the problem that the availability of material for fracture testing is sometimes limited. However, NPPs generally have a large number of irradiated and previously tested Charpy specimens, so the possibility of

performing further testing with this remnant material is of great practical interest. Such testing can be performed using mini-CT specimens, knowing that one tested Charpy specimen allows the fabrication of a maximum of eight 4 mm-thick mini-CT specimens. This mini-CT testing approach brings several benefits, such as: (a) the direct assessment of fracture toughness rather than the semi-empirical approach based on Charpy measurements; (b) the ability to characterize the local properties of heterogeneous materials; (c) a significant increase in the surveillance monitoring database providing greater confidence in the data; (d) a reduction in the volume of irradiated material needed for characterization; and (e) the possibility for re-orientation of the notch in the base material (e.g., T-L vs. L-T) becomes possible, which is particularly important for older plants that have only L-T orientation data while the current ASME Code uses T-L orientation data.

The purpose of this review is to collect and summarize the available scientific and technical information about testing mini-CT fracture specimens, contribute to the development of this miniaturization technique, and provide insights about the main remaining challenges for testing, evaluation, and standardization efforts. A generic issue with the use of mini-CT specimens is associated with the small size itself. The stress intensity factor is a function of the far-field load and the absolute crack size (i.e., $K_I \sim \sigma_0\sqrt{a}$). Therefore, at a given fracture mechanic load K_I, the relative size of the plastic zone (plastic volume/specimen volume) is larger in mini-CTs as compared to larger specimens. Consequently, the violation of the small-scale yielding criterion (and thereby the loss of constraint) starts at lower K-values in mini-CTs, reducing the measuring capacity of mini-CT specimens compared to larger specimens. The implications of this for MC testing are addressed in Section 2.5.

2. Experimental Challenges Presented by the Mini-CT

2.1. The Geometry of Mini-CT Specimens

CT specimens are one of the most common types of standardized specimens used in fracture mechanics testing. The geometry provides an efficient use of the tested material, with the majority of the sample volume used to establish a controlled stress state at the crack tip during loading. However, the miniaturization of CT specimens entails a series of specific testing challenges that are discussed next. This review focuses on 4 mm-thick CT specimens, which may be found in the literature under different names, the most common being mini-CT (the one used in this document), 0.16T-CT, or MCT specimens.

Principally, two different mini-CT geometries have been proposed in the literature, although some minor modifications may be found and will be mentioned in this document where necessary. Figure 2 shows both geometries, also showing a comparison between mini-CT specimens and larger CT specimens (Figure 2b). The first one is the reduced normalized geometry for the CT specimen given by the ASTM E1921 [3] standard: its dimensions are $10 \times 9.6 \times 4$ mm^3 (e.g., [7]). Here, it is important to note that the 2021 version of the standard ASTM E1921 [3] permits the use of this mini-CT geometry for the MC characterization. The second geometry is designed to capture directly the geometry of the Charpy specimen: its dimensions are $10 \times 10 \times 4.2$ mm^3 (the thickness actually ranges between 4 and 4.2 mm) (e.g., [8]). The latter has the advantage of simplified machining, which may be especially important with irradiated materials, although it does not accurately reflect the geometry established by the ASTM E1921 standard [3]. Nevertheless, the literature suggests that this geometric discrepancy does not significantly affect the fracture toughness results, given that the differences in the crack tip stress conditions are small [8,9]. Although it is not clear which geometry will be predominant in the future, in the present review, the specimen that strictly complies with the requirements of the standard ASTM E1921 [3] ($10 \times 9.6 \times 4$ mm^3) will be referred to as (standardized) mini-CT, while the $10 \times 10 \times 4.2$ mm^3 geometry will be referred to as modified mini-CT. Figure 2b shows different CT specimen sizes, including mini-CTs.

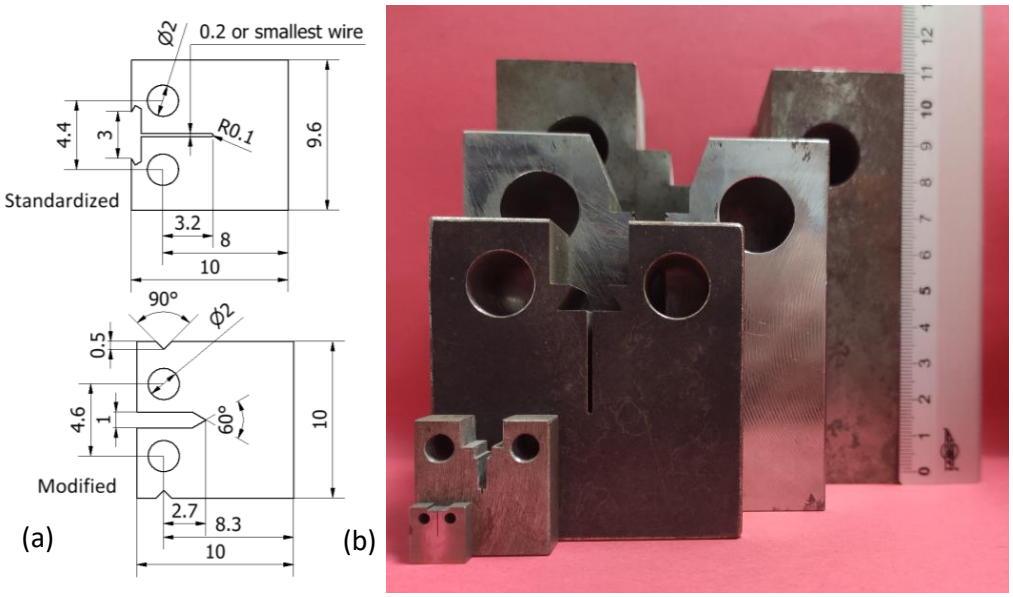

Figure 2. (**a**) Standardized mini-CT vs. modified mini-CT (dimensions in mm); (**b**) image showing the scales of different CT specimens and a standardized mini-CT.

Regarding the standardized mini-CT specimen, ASTM E1921 [3] permits three different CT specimen configurations. However, in practice, only the one without a cut-out section (derived from ASTM E399 [10]) has been employed for mini-CTs due to the difficulty of mounting a clip gauge inside the mini-CT specimen to directly measure the load-line displacement; the purpose of the other two specimens with cut-out sections (see Section 2.2 for further discussion) is to allow room for a clip gauge to measure load-line displacement. One advantage of ASTM E1921 [3] is that it does not establish a specific specimen size, but rather all the dimensions are set relative to the specimen thickness, B. Here, it is important to note that, following [3], the required tolerance of all the dimensions is ± 0.013 W, corresponding to ± 0.1 mm for mini-CT specimens, and the maximum clearance between the pin and the hole is 0.02 W (0.16 mm for mini-CT specimens). Finally, the maximum allowable starter notch dimension shall not exceed 0.063 W, which is about 0.5 mm for mini-CT specimens.

2.2. Load Line vs. Front Face Displacement

As mentioned above, an important topic that affects the geometry of the mini-CT specimen is related to the location at which displacement is measured during fracture tests. Clip gauges may be placed either on the load line (LL) or at the front face (FF) position. Given that mounting a clip gauge inside mini-CTs is generally not feasible, Scibetta et al. [11] proposed a method to measure the LL displacement outside of the mini-CT specimen using a dedicated clip gauge. Its main contribution is related to the use of notches on the top and bottom surfaces of the specimen to allow a clip gauge with sharp razor blades to be placed at the LL position. This technique was also employed by Sokolov [12], who determined that external clip gauges improved the reliability and sensitivity of the measurements when compared to those derived from integrated front-face cut-off notches, such as those suggested in [13–15]. The literature distinguishes two main advantages of using this external LL measurement location: (a) the simplicity of handling such a small specimen and clip gauge in the hot cell or other remote conditions, and (b) more rigidity of the specimen in the region of the loading pins. As a disadvantage, the resulting measurements could be affected when plastic deformation occurs in the vicinity of the pins [8]. Chaouadi et al. [8] compared the displacement measurements on the FF (v_{FF}) versus the LL (v_{LL}). The load-displacement test records of two specimens with medium and high toughness were compared, showing that they lead to comparable K_{Jc} values. Besides, the ratio between

the two measured displacements was about 0.72, in close agreement with those values suggested in the literature (e.g., [16,17]).

As for the FF displacement, ASTM E1921 [3] allows this measurement technique by applying a conversion factor (R) of 0.73, as an alternative to measuring the LL displacement. This conversion factor was derived by Landes [16] from conventional CT specimens by using Equation (3):

$$R = \frac{v_{LL}}{v_{FF}} = \frac{a/W + r \cdot (1 - a/W)}{a/W + r \cdot (1 - a/W) + X/W} \quad (3)$$

where r is the ratio of the distance between the crack tip and the rotation center to the ligament size, and X is the offset between the front face and load line. Landes recommended the value of r = 0.33 and demonstrated that the sensitivity of R on r (dR/dr) is moderate. The conversion factor of R = 0.73 for a standard CT specimen with a/W = 0.5 and X/W = 0.25 corresponds to r = 0.352. In practice, the pre-cracking procedure will not always result in the ideal value of a/W = 0.5; the allowable range is 0.45 to 0.55 [3]. With r = 0.352, this corresponds to a conversion factor range of R = 0.72 to 0.74. In case of deviations from the standard geometry with X/W > 0.25 (e. g. for better applicability of extensometers at FF), the conversion factor R can be significantly affected (e.g., X/W = 0.375 → R = 0.64). Therefore, the evaluation of R with Equation (3) is preferable to a constant value of R = 0.73.

Miura et al. [17] investigated both the conversion factor and the rotation center location factor for mini-CT specimens. Finite element analyses were performed considering three material models with different plastic hardening behaviors. The conversion factor converged within the range of 0.73 to 0.75, and the point of rotation was located at the center of the ligament during loading. These analytic results were then examined using an experimental dataset of mini-CT specimens. The effect of selecting the conversion factor either as 0.73 or 0.75 had a minor impact on the evaluation of the fracture toughness and the estimated T_0 value.

2.3. Side Grooving

In fracture mechanics tests, the specimens are often side grooved to ensure that the crack front after precracking meets the straightness criteria of the testing standards and to improve the uniformity of the stress state along the crack front. However, this technique was found to have little effect on mini-CT specimens [8,18,19] as long as testing is performed within the DBTR. Wallin et al. [19] demonstrated that side grooving has a minor effect on the location of cleavage initiation, although further experimental evidence is warranted. On the other hand, side grooving inherently reduces the measurement capability of the specimen, which is already low in miniature specimens. Yamamoto et al. [18] analyzed the statistical distribution of the data sets with and without side grooving, resulting in a Weibull modulus of 5.1 and 5.5, respectively, thus concluding that side grooving does not affect significantly the statistical distribution of fracture toughness.

2.4. Crack Front Curvature

One challenge when using miniature specimens is generating a sufficiently straight crack front during fatigue pre-cracking. The stress state along the crack front tends to promote fatigue crack growth at the center of the specimen, and the resulting crack front is generally parabolic. In addition, the residual stress state, variation in material properties, or machine misalignment can cause uneven crack growth, resulting in a slanted crack front. For curved crack fronts, the variations in the J-integral and the constraint conditions along the crack front can differ from those existing in straight cracks, which is the crack geometry on which the equations in ASTM E1921 [3] are based.

Lambrecht et al. [20] studied the effect of crack curvature on the T_0 results obtained using mini-CT specimens. They observed a negligible effect of crack front straightness on T_0 by comparing the T_0 values obtained with valid and invalid crack front curvatures, as defined by ASTM E1921 [3]. They also suggested discarding the outermost points from the crack front curvature assessment, something later adopted by ASTM E1921-21 [3].

Lindqvist et al. [21] investigated the effect of crack front curvature on fracture toughness within DBTR by using numerical and experimental methods. The results supported the relaxation of the curvature acceptance criterion proposed by ASTM E1921 [3]. For the investigated crack front curvatures, the effect of curvature on T_0 was smaller than the uncertainty of the T_0 estimations. The authors concluded that curved crack fronts tend to have slightly higher T_0 values, which is conservative.

2.5. Temperature-Related Issues

At low test temperatures, the freezing of the specimen, extensometer, and clevis may affect the experimental measurements. Ice on the clevis and the specimen hinder the connection between the specimen and the extensometer, and this sometimes leads to load-deflection measurements that do not reflect specimen behavior. Furthermore, the possible change in the electric signal of the extensometer needs to be compensated at low temperatures. This phenomenon was studied in an interlaboratory study [14], where tests were carried out with a clip gauge set in the front face of the specimens. It was found that at −150 °C, the clip gauges tended to provide about 3 to 7% larger readings than the actual values due to the change in the electric resistance of the extensometer. Since the linearity between the signal change and the deflection change was maintained, a temperature-dependent coefficient was used for converting the electric signal into the deflection measurement at low temperatures.

On the other hand, the test temperature has to be monitored and controlled on the specimen surface, as established by ASTM E1921 [3]. However, some authors found difficulties in welding a thermocouple on the surface due to specimen size restrictions, and additionally, the effect of heat input on fracture toughness is not clear for such small specimens. Therefore, several authors (e.g., [7,18]) decided to control the test temperature by means of a thermocouple welded on the surface of the clevis. The temperature difference between the specimen and the clevis was found negligible after holding the specified temperature for at least 15 min [7]. However, other work [22] decided to monitor directly the test temperature with a thermocouple attached to the surface of the specimen.

Another important topic when dealing with the mini-CT specimen is determining the number of specimens required to obtain a valid T_0 value, which is intrinsically related to the temperature range selected for the tests. It is necessary to mention the limitations on testing conditions imposed directly by the ASTM E1921 standard [3]. Two of the most important restrictions are the $T_0 \pm 50$ °C testing temperature range, and the $K_{Jclimit}$ value for the fracture toughness results (see orange curve in Figure 1), which is the limiting value for data censoring:

$$K_{Jclimit} = \sqrt{\frac{E \cdot b_0 \cdot \sigma_y}{30 \cdot (1 - \nu^2)}} \quad (4)$$

where b_0 is the remaining ligament, σ_y is the material yield strength, E is the elastic modulus, and ν is the Poisson's ratio. $K_{Jclimit}$ ensures that the remaining ligament has sufficient size to ensure high constraint conditions at the crack front and that small-scale yielding conditions are met. The remaining ligament, b_0, is proportional to the thickness of the specimen, thus, as shown in Equation (4), the smaller the ligament, the smaller the $K_{Jclimit}$. Hence, small specimens such as mini-CTs have low $K_{Jclimit}$ values, which forces testing at rather low temperatures to ensure that most measured K_{Jc} values fall below $K_{Jclimit}$; this reduces the temperature range over which mini-CT tests can be conducted.

Another aspect that conditions the $K_{Jclimit}$ is the material yield strength. In this sense, Sugihara et al. [23] analyzed the effect of this material property in the $K_{Jclimit}$ of irradiated materials, and therefore its impact on the validity window of the MC approach. For irradiated conditions for the same test temperature, σ_y is higher than in unirradiated conditions. On the other hand, the change in T_0 due to irradiation embrittlement leads to higher test temperatures for irradiated materials than for unirradiated materials. For these reasons, if the decrease in σ_y by increasing the test temperature is greater than the

increase in σ_y caused by irradiation, the σ_y of the irradiated material may be lower than that of the unirradiated material at the corresponding test temperatures. Therefore, $K_{Jclimit}$ may be even lower in irradiated conditions than in unirradiated conditions. The authors studied this effect by using literature data [24] finding no significant tendencies for this particular case.

Regarding the test temperature, ASTM E1921 [3] recommends the selected temperature be close to that at which the K_{Jcmed} value is approximately 100 MPa·$m^{0.5}$ for the specimen size being used. Based on that, Tobita et al. [22] proposed that for mini-CT specimens, the test temperature equivalent to 100 MPa·$m^{0.5}$ would be given by the K_{Jcmed} MC expression together with the corresponding thickness correction, as shown in Equation (5).

$$100 = \frac{\{30 + 70 \cdot \exp[0.019 \cdot (T - T_0)]\} - 20}{\left(\frac{B_{0.16T}}{B_{1T}}\right)^{0.25}} + 20 \quad (5)$$

Clearing for the equation, resulted in $T = T_0 - 29°C$. However, considering that the precision of the test temperature control is ±3 °C, the optimum test temperature to minimize the likelihood of invalid K_{Jc} values (i.e., K_{Jc} values larger than $K_{Jclimit}$) was selected as $T = T_0 - 32°C$.

Moreover, Miura et al. [7] reported, for the unirradiated mini-CT specimens, the range of temperatures that would lead to reducing the invalid data due to $K_{Jclimit}$, improving the efficiency when obtaining valid (non-censored) data. They observed that the ratio of valid data (the number of uncensored values to the total number of tests) for the mini-CT specimens increased when $T\text{-}T_0$ was reduced and reached unity when $T\text{-}T_0$ was less than −30 °C. This trend agrees well with the reference curve from ASTM E1921 [3], which was obtained for PCCv (pre-cracked Charpy) specimens. Therefore, the recommendation was to test mini-CT specimens within the range of $-50\ °C \leq T - T_0 \leq -30\ °C$. This test temperature range was subsequently confirmed on materials in both irradiated and unirradiated conditions [8,23,25].

In terms of the number of specimens, the ASTM E1921 standard [3] suggests a minimum number of valid tests ranging from 6 to 9 specimens, depending on the testing temperatures, in order to determine a valid T_0. At the same time, it is well known that the uncertainty in T_0 determination increases when the lower shelf is approached, which is otherwise necessary (as shown above) to obtain a sufficient number of uncensored K_{Jc} data. This phenomenon may be countered by increasing the number of tests since the uncertainty of T_0 is inversely proportional to the square root of the number of uncensored specimens, as shown in Equation (6).

$$\sigma_{T0} = \left(\frac{\beta^2}{r'} + \sigma_{exp}^2\right)^{1/2} \quad (6)$$

where β is the sample size uncertainty factor determined following Section 10.9.1 in ASTM E1921 [3], r′ is the total number of uncensored data used to calculate T_0 and σ_{exp} is the contribution of experimental uncertainties, usually taken as 4 °C.

In this regard, Chaouadi et al. [8] determined the minimum number of specimens leading to a reliable T_0 value, assuming that this will be the one calculated using the largest number of specimens. For this purpose, a set of mini-CT tests of different materials was examined, and the transition temperature was iteratively calculated as the number of tests used in the calculation increased. The analysis determined that the T_0 stabilized within ±2 °C after using about 16 specimens in the calculation and found that the minimum number as required per ASTM E1921 [3] is mostly between 8 and 10 specimens, or even more. It should be noted that this minimum number is based on experimental data for materials with known T_0. Thus, for materials that are characterized solely by mini-CT, a larger number of specimens may be required.

Another criterion imposed by ASTM E1921 [3] is the ductile crack growth (DCG) limitation. This criterion established that DCG cannot exceed either 0.05 ($W\text{-}a_0$) or 1 mm,

being in practice around 0.2 mm for mini-CT specimens. This is particularly important for low upper-shelf (LUS) materials. As was reported in several works [25–27], this type of material may exhibit DCG at temperatures near T_0, complicating the selection of testing temperatures. Therefore, the authors recommended testing more than 15 specimens to properly carry out an MC evaluation for LUS materials.

In summary, to obtain valid results, it is recommended to test at least 30 °C below the final T_0, increasing the chances of obtaining non-censored results (see the shaded area in Figure 3). Additionally, the testing temperature cannot be below ($T_0 - 50$ °C) according to the requirements of ASTM E1921 [3] and JEAC4216 [4], and, finally, T_0 is not known exactly beforehand. Figure 3 shows the ratio of valid data (non-censored test results to the total number of tests) versus the test temperature ($T - T_0$) in a number of experimental results. Each point represents a set of experimental results performed on a given material at a given temperature. It can be observed how the range $-50\ ^\circ\text{C} \leq T - T_0 \leq -30\ ^\circ\text{C}$ maximizes the ratio of valid data. The figure also shows the ASTM E1921 [3] requirement of valid data, which depends on the test temperature and the resulting T_0, revealing how it fits the experimental results. Finally, the red line in Figure 3 shows a proposal for a hyperbolic tangent best-fit curve (non-linear least squares):

$$f(x) = A + B \times \tanh((x - C)/D) \tag{7}$$

where A, B, C, and D are the four parameters required for the adjustment of the curve, which takes values of 0.802, −0.196, −17.16, and 11.06, respectively. The curve reveals how the ratio of valid data is close to 1 as long as $T - T_0 \leq -30$ °C, in agreement with the results shown above (e.g., [7,8,23,25]).

Recently, efforts have been made to address these issues. Yamamoto et al. [28] published a paper that aims to extend the validity temperature range below ($T_0 - 50$ °C) by defining new criteria that allow the inclusion of data in the MC evaluation that otherwise would be rejected.

To conclude with the temperature-related issues, it is clear from the information summarized here that knowing an initial estimation of T_0 is beneficial, given that the above discussions assumed that the T_0 value was already known for the studied material. In many situations (e.g., when surveillance data are available), T_0 can be estimated from existing Charpy data (e.g., [3,23,25]), but this will not be possible in all situations. When Charpy impact transition curves are available, the ASTM E1921 [3] standard provides a procedure for selecting a test temperature (T) in the neighborhood of T_0. Indeed, the ASTM E1921 [3] standard proposes the following relationship between test temperature, T, and T_{41J}:

$$T = T_{41J} + C \tag{8}$$

where the constant C is given for various specimen thickness values that can be fitted with the following equation:

$$C\ = 14.845 \times \ln[\text{thickness(mm)}] - 71.8\ ;\ ^\circ\text{C} \tag{9}$$

For the mini-CT specimen, this equation provides $T = T_{41J} - 51$ °C [7]. However, this estimate does not guarantee that the resulting test temperature is appropriate for mini-CT specimens.

Equation (8) is based on the work by Sokolov and Nanstad [24], who studied the relationship between T_0 and T_{41J}. The authors derived the following well-known expression:

$$T_0 = T_{41J} - 24\ ^\circ\text{C} \tag{10}$$

The general trend, according to the reviewed literature, is that the Sokolov correlation [24] can be used, as shown in Figure 4.

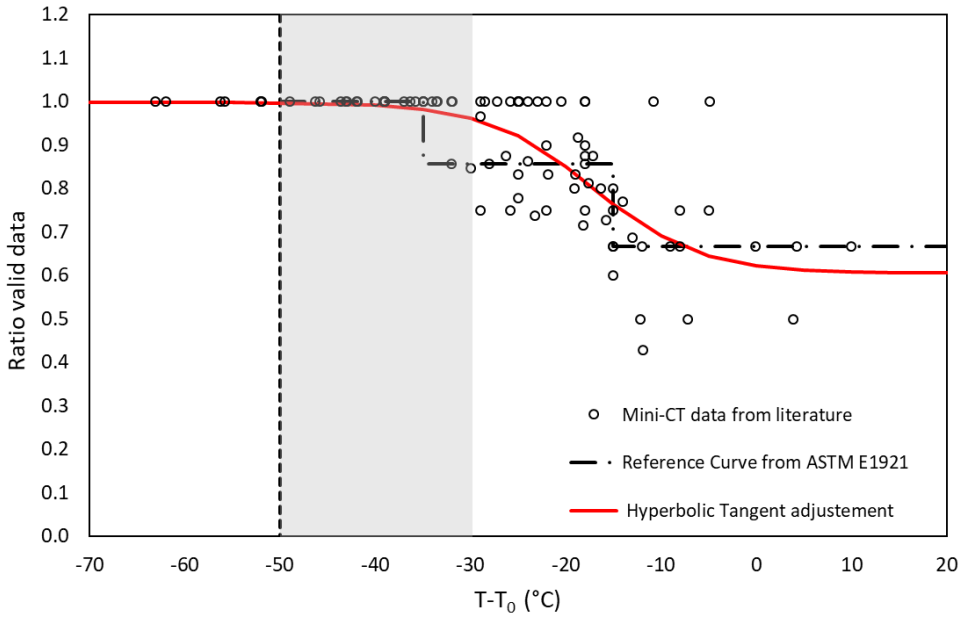

Figure 3. Relation between the ratio of valid data vs. $(T - T_0)$ for mini-C(T) specimen. T is the testing temperature. Data from: [7–9,12–14,22,23,26,29–34].

As was mentioned above, Tobita et al. [22] intended to define an initial test temperature by providing a K_{Jcmed} value of 100 MPa·$m^{0.5}$ by the following equation: $T = T_0 - 32$ °C. Thus, considering Equation (10), they suggested the following equation to select the test temperature for mini-CT specimens:

$$T = T_0 - 32\ ^\circ C = T_{41J} - 56\ ^\circ C \quad (11)$$

Further refinement of Tobita's approach has been documented in subsequent publications by JAEA [30,32,35].

More recently, Yamamoto et al. have demonstrated that even with an uncertain estimation of the initial test temperature, which is possible due to the uncertainty of Equation (10), test temperature selection for a few subsequent specimens may help to quickly recover from the issue [36]. They demonstrated that even if the initial test temperature is less than optimal due to an uncertain pre-estimated T_0, which was defined as up to a maximum deviation of 40 °C from the true T_0, the resultant success rate of T_0 evaluation using N = 12 or fewer specimens is quite high (98% or more) (see Table 1) if their proposed test temperature selection procedure is used.

Table 1. Influence of error in initial T_0 guess on the success rate of valid T_0 evaluation with N=12 or fewer specimens [36].

$\sigma_{YS(RT)}$, MPa	True T_0, °C	T_0 Guess − True T_0, °C				
		−40	−20	0	20	40
400	−50	97.9%	98.6%	99.1%	98.6%	98.5%
500	0	99.4%	98.6%	99.8%	98.9%	99.5%
600	50	100.0%	100.0%	99.9%	99.6%	99.9%

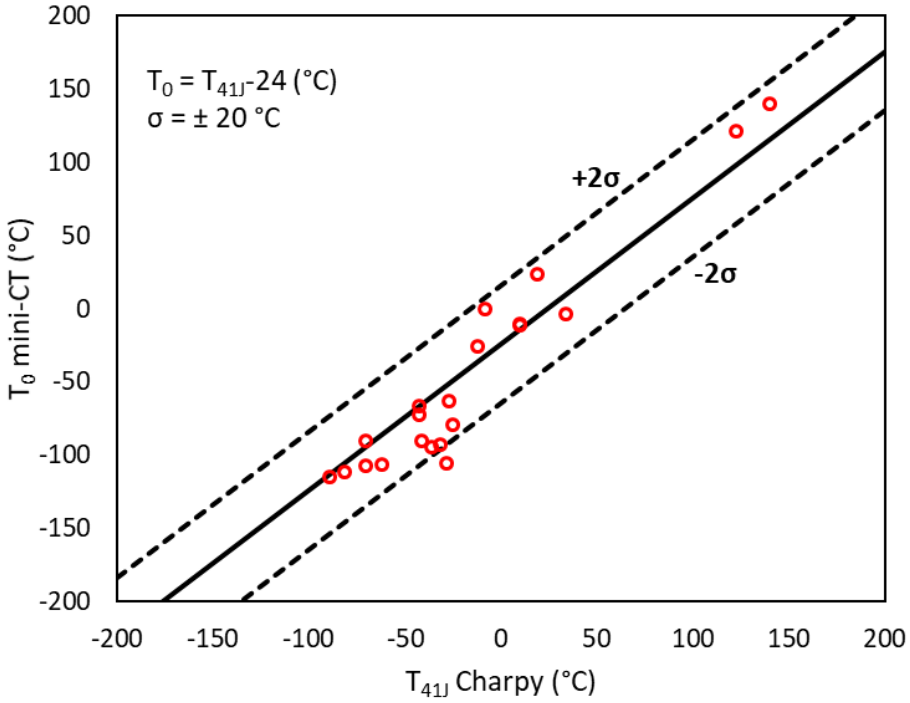

Figure 4. Correlation between mini-CT T_0 values and T_{41J} values obtained from Charpy testing. Data were taken from [7,8,11,14,22,23,30,33,35,37,38].

2.6. Loading Rate during Fracture Testing

Regarding the loading rate during the fracture testing, ASTM E1921 [3] recommends a dK/dt range of 0.1 to 2.0 MPa $\sqrt{m}/s$. Hall and Yoon [39] evaluated the loading rate dependency of T_0 values determined from PCCv specimens and other larger CT specimens for eight different materials, using the following equation:

$$T_{0R2} = T_{0R1} + B \cdot \ln(R2/R1) \quad (12)$$

where R1 and R2 are the loading rates and B, varied from 2.2 to 5.7, depending on the material. This loading rate dependency was studied in [22] for mini-CT specimens, revealing a similar behavior to that observed in larger specimens. The higher loading rates generated slightly higher T_0 values, and this tendency was almost the same for the larger specimens. In [15], it was shown that due to the proportionally larger plastic deformation developed in mini-CT specimens during fracture tests, the loading rate change in mini-CT specimens is, therefore, larger than that developed in larger specimens. However, in spite of this observation, no specific dependency of T_0 with the loading rate could be established for mini-CTs as long as the loading rate meets the ASTM E1921 [3] validity range ($0.1 < dK/dt < 2$ MPa·$m^{0.5}$/s).

3. Results on Unirradiated and Irradiated Steels

The DBTR of ferritic steels has been widely analyzed over the years. The main engineering tool developed to characterize the material fracture toughness within the DBTR is the MC approach [1,2], which is standardized in ASTM E1921 [3] and widely described elsewhere (e.g., [1,2]).

One of the first works related to mini-CT specimens was reported by Miura et al. [7]. They focused on two typical Japanese RPV steels, SFVQ1A forging, and SQV2A plates of two different heats. They carried out at least 6 to 8 tests per temperature, thus allowing a comparison between the single-temperature method and the multi-temperature method [3]. No significant effect was found in the T_0 evaluation method, the maximum difference being

4.7 °C. A comparison among T_0 values obtained from different CT sizes (4T, 2T, 1T, 0.4T, and 0.16T) showed a maximum deviation from the average of 4.8 °C, 4.5 °C, and 10.5 °C for SFVQ1A, SQV2A Heat 1, and SQV2A Heat 2 materials, respectively. Therefore, they concluded that T_0 can be accurately determined using mini-CT specimens.

A three-year round-robin was organized by the Central Research Institute of Electric Power Industry (CRIEPI) in Japan to verify the reliability and robustness of obtaining T_0 by means of mini-CT specimens. The first and second round robin tests [13,15] were performed on the SFVQ1A steel. The average value of the ten T_0 evaluations carried out within the first two years of the program was −102 °C, which agrees well with the T_0 values obtained with larger specimens (−91 °C to −103 °C). Besides, it was very close to the T_0 value obtained by Miura et al. [7], which, when applying the multi-temperature evaluation, resulted in a T_0 of −101 °C. Thus, the first and second round robin tests [13,15] suggested that the T_0 evaluation technique using mini-CT specimens is fairly robust.

The final stage of the mini-CT round-robin program [14] carried out on unirradiated SQV2A steel showed that six laboratories were able to determine T_0 within the expected scatter range. The fracture tests were carried out as blind tests, which means that detailed material information, such as the type of material, estimated T_0, and existing fracture toughness data for the material, were not provided to the laboratories beforehand. Participants independently selected the test temperature based on the full Charpy curve of the tested material. Although the test temperatures selected by the various laboratories varied from −120 to −150 °C, the obtained T_0 values with mini-CTs were reasonably consistent with each other; the maximum difference among participants being 16 °C. The T_0 determined using all of the mini-CT test results was equal to −115 °C. This value is in good agreement with the T_0 calculated by Miura et al. [7].

Tobita et al. [22] performed an extensive experimental campaign with five types of SA533B C1.1 RPV steels with different ductile to brittle transition temperatures. All data sets gave valid T_0 values, showing a good relationship between the T_0 obtained from mini-CT specimens and those determined from 1T-CT specimens; the maximum deviation between the 1T and mini-CT T_0 values was 13 °C for steel JRM. This database was posteriorly expanded by Takamizawa et al.'s [37] work and found a difference between mini-CT results and 1T-CT results not exceeding 10–15 °C.

The applicability of mini-CT samples with the MC approach has been confirmed for several Japanese base metal RPV steels. However, it was necessary to extend and ensure the applicability of this methodology to weld metals, which is of great interest to guarantee the safety of NPPs during long-term operation (LTO). Generally, RPV weld metals are recognized as homogeneous materials, but weld metals often exhibit inhomogeneity in multi-pass bead welding. Likewise, the HAZ in the base metal beside the weld fusion line is also one of the materials to be investigated in the surveillance programs. Since the available volume of the HAZ region is limited, the utilization of small specimens is important [29]. In this sense, several experimental campaigns have been completed in the last decade. Yamamoto et al. [18] completed fracture tests on SQV2A weld metal. The T_0 values of this weld metal obtained with mini-CT and 0.5T-CT specimens demonstrated excellent agreement, both generating a T_0 value of −77 °C. Additionally, a set of mini-CT specimens were tested with side grooves, resulting in a T_0 of −80 °C. The fixed value of C = 0.019 in the MC (see Equation (1)), which defines the shape of the K_{Jcmed} curve, was evaluated as a variable. The parameter C was calculated as 0.018 and 0.021 for the weld metal and the base metal, respectively, demonstrating that both the weld metal and the base metal may be evaluated following the MC recommendation. Subsequently, this SQV2A weld metal was investigated in an international round-robin program composed of four participants [40]. All of them obtained a valid T_0 value, with a maximum difference among them of 14 °C, which was reasonably small in comparison with the previous round-robin [14].

Yamamoto et al. [29] prepared an experimental campaign with two plates of SQV2A steel and different sulfur contents (denoted as Low S and Mid S) that were joined to each other with SQV2A weld metal by the submerged arc welding method. In total, five data

sets were obtained with mini-CT specimens, two from the base materials, one from the weld metal, and two from the corresponding heat-affected zones. All data sets provided a valid T_0 value. However, when comparing the results with the T_0 values determined from 0.5T-CT specimens, the difference between the mini-CTs and the 0.5T-CTs observed in HAZ materials was larger than in the other materials. A difference of 25 °C and 10 °C was found in Low S HAZ and Mid S HAZ, respectively. Micrography analysis of the HAZ specimens (6 mini-CT and 6 0.5T-CT specimens) showed that the width of the HAZ region varied from 2.7 mm to 3.3 mm among specimens. Here it is important to note that mini-CT specimens have dimensions of 10 mm × 9.6 mm, while the 0.5T-CT specimens have dimensions of 31.25 mm × 30 mm, so it is evident that in the mini-CTs a large part of their volume is composed by the HAZ material, thus allowing a more precise characterization of the fracture of this particular zone. In any case, the authors concluded that the large variation of T_0 observed in the HAZ could be caused by the inherent heterogeneities associated with this area.

Chaouadi et al. [8] studied RPV steel 22NiMoCr37 by using the modified mini-CT specimen ($10 \times 10 \times 4.2$ mm^3) in non-irradiated conditions. In addition to the findings mentioned in the previous section, they concluded that the difference in the T T_0 obtained using conventional CTs and mini-CTs is around 12 °C, while in the case of precracked Charpy specimens (PCCv) the difference is 5 °C.

Another fundamental aspect when dealing with mini-CT specimens is the similitude of the cleavage initiation process since the MC is based on the assumption that specimen size does not affect this similitude and the thickness would only cause a statistical effect that can be easily corrected by means of the well-known Equation (2). This issue was examined by Wallin et al. [19] by comparing the location of cleavage initiation sites along the crack front for different specimen sizes and configurations, focusing the effort on mini-CT specimens. The authors determined the cumulative initiation location distribution of several datasets and found that the majority of initiations took place within 40% of the specimen center ($0.3 \leq x/B \leq 0.7$, x being the distance from one side of the specimen and B being the specimen thickness) and, in addition, in about 30% of the center of the specimen, the location initiation probability was uniform. This trend of concentrating the initiation points at the center of the specimen for mini-CT specimens was also assessed for larger (conventional) single-edge notch bend (SENB) and CT specimens. The results confirmed that the specimen size or type has a minimal effect on the distribution of the initiation location sites as long as the requirements of the ASTM E1921 [3] standard are fulfilled.

So far, the review has been focused on the applicability of mini-CT specimens in unirradiated specimens, revealing the success of this technique. Now, the results on irradiated materials are presented.

Ha et al. [30] studied a Japanese A533B class 1 steel, which was named Steel B. Mini-CT specimens were taken from the halves of irradiated PCCv specimens, which were subjected to a neutron fluence of 1.1×10^{20} n/cm^2 at 290 °C. The mini-CT specimens provided a T_0 value of −11 °C, which is slightly higher than that obtained using PCCv specimens, −24 °C. Here, it is worth mentioning that the IAEA reported a bias of around 10 °C between the CT specimen type and PCCv specimens [41].

Yamamoto [31] reported an inter-laboratory effort to evaluate European JRQ material irradiated with a fluence of 1.85×10^{19} n/cm^2 at 286 °C. All the laboratories could obtain a valid T_0 value from the given number of mini-CT and PCCv specimens in both unirradiated and irradiated conditions. The results under unirradiated conditions demonstrated a good agreement in T_0 values, −68 °C for the mini-CT specimen and −67 °C for the PCCv specimen. Despite these valid T_0 results, the JRQ material demonstrated a wide fracture toughness scatter. An excessive number of K_{Jc} values (13% for mini-CTs and 25% for PCCv specimens) were located outside the MC bounds. This trend has already been observed in previous projects, which indicated that the large dispersion of the data could be due to the inhomogeneity of the material. Regarding the irradiated state, the laboratories produced

T_0 values of 32 °C and 40 °C with mini-CT specimens, which were in good agreement with the resulting T_0 of 44 °C obtained using PCCv specimens.

Sugihara et al. [23] evaluated Japanese steel SFVQ1A subjected to a neutron fluence of 7.2×10^{19} n/cm^2 with mini-CT specimens and with 0.5T-CT specimens. Both data sets provided a valid T_0 of −1 °C for the mini-CT specimens and 8 °C for 0.5T-CT specimens. Thus, a difference of 9 °C was found, although the standard deviations (7.8 °C for mini-CT and 6 °C for 0.5T-CT) well overlapped each other.

After demonstrating the suitability of mini-CT specimens to characterize the JRQ material both in baseline and irradiated conditions [31], the same group (two laboratories) analyzed the possibility of evaluating the through-wall fracture toughness distribution with mini-CT specimens [32]. For this purpose, a block of JRQ steel was sliced into 13 layers, and the inner four layers (01J, 02J, 03J, and 04J) were used for the evaluation. The inner layer (01J) received a maximum neutron fluence of 5.38×10^{19} n/cm^2, which was attenuated to 2.54×10^{19} n/cm^2 at the 04J layer (60 mm from the inner surface). The irradiation temperature was 286 °C. Two more inner layers (01J, and 02J) were tested in the unirradiated conditions by one laboratory, providing (using mini-CTs) a T_0 of −121 °C and −115 °C for 01J and 02J, respectively. These values deviate by 3 °C and 8 °C, respectively, when compared to the results obtained with PCCv specimens. For the irradiated material, the T_0 results obtained by the two labs were comparable in layers 01J and 03J, but 02J showed a difference of 29 °C, which was close to $T_0 + 2\sigma$ (but still a bit larger) for the number of tested specimens. In conclusion, the use of mini-CT specimens was shown to be suitable to analyze the toughness distribution through the vessel wall. The use of specific fracture toughness values obtained at the inner surface (where neutron fluence is higher) may improve structural integrity assessments (e.g., pressurized thermal shock evaluations).

Ha et al. [35] also analyzed highly neutron-irradiated materials. In this case, three types of Japanese RPV steels were used, designated as Steel B, 3B, and 5B. Different levels of neutron fluence were applied: 11.3×10^{19} n/cm^2 for Steel B, 5.4×10^{19} n/cm^2 for 3B, and two fluence levels for 5B, the lower fluence (5BL) was 5.6×10^{19} n/cm^2 and the higher fluence (5BH) was 10.4×10^{19} n/cm^2. All the obtained T_0 values were valid. Finally, the specimen type effect was studied with Steel B in irradiated conditions: the T_0 value obtained through mini-CTs was about −12 °C, while in the case of PCCv specimens T_0 was −25 °C, resulting in a difference of 13 °C.

A collaborative program [25–27,42] was performed to characterize weld WF-70 material in both baseline and irradiated conditions. This low upper shelf Linde 80 weld had been previously characterized within the Heavy Section Steel Irradiation (HSSI) program with different types of larger C(T) specimens [43]. This program was performed in the 1990s, so the T_0 values reported here were recalculated from the original K_{Jc} data using the procedures of the current version of the ASTM E1921 [3] standard, obtaining T_0 values of −60 °C and 29 °C in unirradiated and irradiated conditions, respectively. The WF-70 material was then evaluated with mini-CT specimens by one laboratory in the unirradiated condition [12], resulting in a valid T_0 of −53 °C. The same laboratory evaluated the material in irradiated conditions [25], providing T_0 values of 2 °C or 12 °C, depending on the censoring criterion used for specimens with excessive ductile crack growth ($K_{Jclimit}$ vs. $K_{Jc\Delta a}$, see [25] for further details). Moreover, two additional laboratories tested the weld material by using the standard mini-CT specimen in irradiated conditions [27]. One of the laboratories could not obtain a valid T_0 value but provided a tentative T_{0Q} (provisional reference temperature [3]) of 31.3 °C. The other one obtained a valid T_0 of 34.8 °C. The combination of both data sets yielded a valid T_0 of 31.5 °C. All these data, in addition to those developed by a third laboratory, were analyzed as part of an inter-laboratory study [26]. T_0 in the irradiated condition varied between 13.2 °C and 17.5 °C, depending, again, on the censoring criterion.

Lambrecht et al. [9] investigated a series of mini-CT specimens taken from an A508-type weld metal in unirradiated and irradiated states. The steel was irradiated to a neutron fluence of 5×10^{19} n/cm^2 at 290 °C. In this study, modified mini-CT specimens with 20%

side grooves were employed. Fully valid T_0 values were obtained for the two conditions: −80.9 °C and −32.8 °C for unirradiated and irradiated conditions, respectively.

Uytdenhouwen et al. [33] studied the A508 Cl.2 RPV steel in irradiated and unirradiated conditions by means of mini-CT specimens. In this case, modified specimens were used, resulting in a T_0 of −88.1 °C for unirradiated material, which is similar to the −87.4 °C obtained with the 0.5T-CT specimen and to the −95.2 °C obtained with PCCv specimens.

Chen et al. [34] evaluated the applicability of mini-CT specimens to characterize the DBTR of two reduced activation ferritic martensitic (RAFM) steels proposed for fusion blanket applications, the EUROFER97 batch-3, and the F82H-BA12 steels. They did not obtain valid T_0 results, but they did observe that the resulting T_{0Q} was 40 °C lower for EUROFER97 batch-3 and 15 °C lower for F82H-BA12 when testing was performed on 0.5T-CT specimens with slanted fatigue precracks. In contrast, T_{0Q} was only 11 °C lower for EUROFER97 batch-3 and 4 °C higher for F82H-BA12 when testing was performed on mini-CT specimens with slanted fatigue precracks. One implication from this observation is that mini-CT specimens may be less sensitive to test imperfections and yield more consistent T_{0Q} values.

Han et al. [44] also studied the F82H RAFM steel, showing a negligible effect on the T_0 value of 1 °C when compared with the 1T-CT specimen.

Sokolov [45] studied KS-01 weld material in unirradiated and irradiated conditions. The T_0 derived from testing mini-CT specimens in the unirradiated condition was −9 °C, compared to −26 °C reported for a combination of 1T-CT, 0.5T-CT, and PCCv specimens. The T_0 temperature derived from irradiated mini-CTs was 153 °C, compared to the 139 °C reported for a combination of 1T-CT and 0.5T-CT specimens.

In summary, Figure 5 shows a comparison between the T_0 values obtained with large conventional specimens and those obtained using mini-CT specimens. The majority of the values gathered from the literature, including unirradiated and irradiated materials, are located between the bands of ±15 °C, as shown in the graph. On average, considering all the data reviewed here, the difference between T_0-mini and T_0-conventional specimens is less than −1 °C. Thus, in general, the values of T_0 obtained with mini-CT specimens are in good agreement with those obtained with larger specimens, demonstrating the robustness of mini-CT MC characterization.

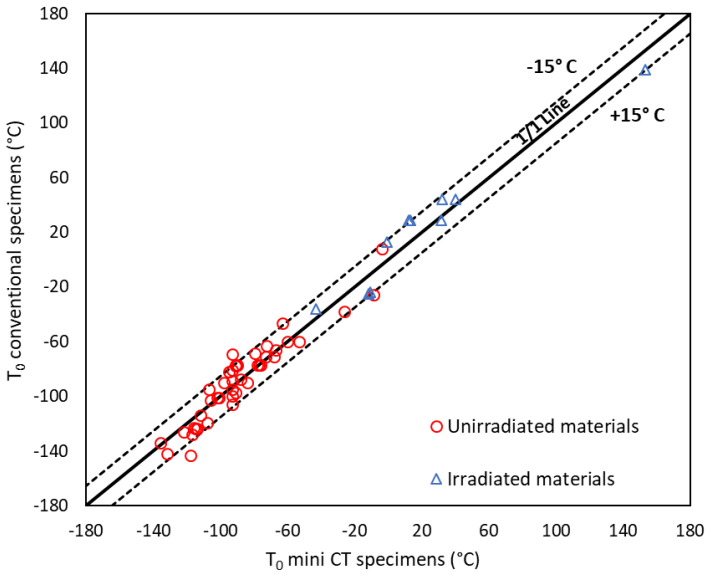

Figure 5. Comparison between T_0 values of unirradiated materials determined from conventional specimens and T_0 values obtained using mini-CT specimen. Results from: [7–9,11–15,18,20,22,23,25–27,29–31,33–35,37,38,40,42,44–46].

4. Regulatory Aspects

4.1. Initial MC Applications and Applicability Concerns

The size effect and scatter characterization of Wallin's MC concept were first introduced in 1984 [2,47], followed by Wallin's identification of a temperature dependence that works well for a wide range of ferritic steels in 1993 [48]. The first codification of MC techniques came with the 1997 adoption of the ASTM E1921 testing standard [3] and the 1999 ASME Code Cases that defined an MC-based reference temperature, RT_{T0}, that is the functional equivalent of RT_{NDT} [49–51]. RT_{T0} was moved from these code cases into the ASME Code itself in 2014. Early plant-specific applications of the MC in the USA included the Zion reactors in 1993 [52], and the Kewaunee reactor in 1998 [53,54]. MC was also used in South Korea to demonstrate the continued operating integrity of the Kori Unit 1 reactor in 2007 [55]. Continued regulatory use of MC techniques has occurred for PWR units in the USA having Linde 80 welds in their RPV beltline through the use of the "BAW-2308" approach [56], which allowed better estimation of the unirradiated RT_{NDT} value for Linde 80 welds using master curve results. The BAW-2308 approach has been used for nearly a dozen operating reactors.

During the late 1990s and early 2000s, there were no regulatory or Codes and Standards procedures for the use of MC. At that time, the regulator in the USA published a paper providing its views on MC technology and its applicability to the safety assessment of nuclear RPVs [57]. These authors stated that *"the Master Curve approach is promising . . . , however significant technical, process, and regulatory issues remain to be adequately addressed before full implementation of such an approach can be endorsed by the NRC."* The paper went on to highlight the following issues (direct quotations from [57] appear in italics):

1. *Fracture toughness characterization performed on the actual material in question or an appropriately qualified "surrogate".*
2. *Fracture toughness characterization performed in specimens with adequate constraint and at appropriate loading rates.*
3. *Quantification of the effects of irradiation on the shape (meaning temperature dependence) of the Master Curve.*
4. *Development and finalization of consensus Codes and Standards (ASTM, PVRC, and ASME.)*
5. *Revisions to USNRC rules and regulations governing RPV integrity.*

Item (1) was not directly related to the MC but rather to the long-standing recognition that some early construction plants in the USA did not monitor their limiting beltline material as part of their surveillance programs. The limiting materials were not monitored in some cases due to a lack of specificity in the then-current ASTM surveillance standard, which was attributable to a lack of knowledge in the 1960s and 1970s needed to identify the steels in the RPV beltline most sensitive to irradiation embrittlement. While item (1) also affected conventional RT_{NDT}-based assessments, it was raised by the NRC in the context of potential MC use due to the perception that using the MC would reduce some of the large implicit conservatisms thought to be inherent to RT_{NDT}. Item (1) has been largely resolved over the last 20 years, and moreover, systematic methods now exist to identify groups of similar materials from the large quantities of surveillance data now available [58].

Item (2) reflected concerns about (a) the use in T_0 estimation of what were then called "invalid" data (now referred to in ASTM E1921 and JEAC4216 as "censored" data) and (b) the change from using a dynamic Charpy test approach to a statically loaded fracture toughness test approach as the basis for positioning reference fracture toughness curves. Item (2a) has been addressed thoroughly via the standardization processes associated with ASTM E1921 and JEAC4216; consensus procedures are now well established to ensure the appropriate treatment of censored data. Item (2b) was addressed when the ASME Code moved in the late 1990s from using dynamic crack initiation and crack arrest data to static crack initiation data as the basis for the Code reference fracture toughness curve [59]. Moreover, there was the realization that the magnitude of Charpy shift with irradiation damage is linearly related to T_0 shift, and that the two quantities are generally equal, or nearly so [60]. To the extent that this question remains open, an ongoing effort to develop an

ASME Code Case aims to provide explicit procedures to address embrittlement, including treatment of uncertainties [60].

Item (3) has been resolved through extensive data analyses that show that the fixed Master Curve shape provides a good representation of the temperature dependence of RPV materials through any now foreseeable RPV lifetime [53,61], including steels with irradiation-induced shifts as high as ΔT_0 = 165 °C [62]. While Wallin has presented a version of the MC having a temperature dependence related to both yield strength and T_0 [63], this variation is slight. Within the range of interest for RPV steels, the fixed shape MC continues to provide a good representation of the large collections of data now available. Neither MC testing standard, ASTM E1921 [3] or JEAC4216 [4], has seen the need to adopt the variable temperature dependence of MC from [63].

Concerning Item (4), as mentioned previously in ASTM E1921 [3] and JEAC4216 [4], MC testing standards are now well developed, representing over two decades of continuous improvement. ASME, JEAC, and other MC application standards continue to be developed, as summarized in Section 4.2.

Concerning Item (5), in the USA, the MC has not been adopted as part of any regulatory code or regulatory guidance document; however, the NRC has reviewed and endorsed parts of the ASME Code that use the MC as part of their ongoing processes that adopt the code and code cases as legal parts of the regulatory framework in the USA. The MC has seen legal endorsement by regulators in both Germany [64] and Switzerland [65]. In Japan, JEAC4206 has provisions for using the MC for the evaluation of plant operating limits [66]. While the 2016 version of JEAC4206 has been adopted by the Japan Electric Association, it has not yet been endorsed by the regulatory authority in Japan. The Swiss, German, and Japanese approaches are broadly similar to the ASME RT_{T0} approach, albeit differing in certain specific provisions and in their approaches to setting margins. Section 8.3 of [60] provides a more complete summary of the various approaches.

4.2. Current Activities in the USA

In the USA, considerable effort has been made since 2014 to incorporate MC concepts formally and comprehensively into the ASME Code, including a treatment of embrittlement and uncertainties, as follows:

- Code Case N-830-1: Following a 7.5-year development effort, Revision 1 to Code Case N830 was adopted into the Code in September 2021 following a unanimous and affirmative vote within ASME Section XI, including by the NRC representative [67]. This Code Case provides 5th percentile curves based on MC and extended MC models that can be used as alternatives to allowable toughness models now in the Code. Specifically, N-830 allows users to calculate, based only on knowledge of a T_0 value and the product form in question, the 5th percentile curves for 1T-K_{Jc} (which per this code case may be used as an alternate to K_{Ic}), K_{Ia}, J_{Ic}, and J-R. These toughness curves may be used in assessments of found flaws, to establish safe plant operating limits, and an evaluation of the fracture toughness needed on the upper shelf. The review and approval process associated with this code case included extensive interchange with the NRC to address the regulators' concerns on many topics, including validation and uncertainty treatment. This interchange is fully documented as an appendix to [67].
- Code Case N-914: This code case, which has been under development since 2019 and remains in draft form, provides a consistent and comprehensive methodology to assess embrittlement, including uncertainty treatment, for both conventional code approaches based on Charpy and NDT as well as MC-based approaches [60]. The current technical basis was reviewed by the NRC in 2021, and most questions were addressed. Future revisions of [60] will fully document the interchange with the NRC in the same manner as done with CC-N-830-1. In combination with Code Case N-830-1, Code Case N-914 provides a comprehensive and explicit methodology to use the MC and T_0 in ASME Code assessments.

In the reviews conducted on these two code cases, the NRC asked no questions concerning the use of mini-CT to estimate T_0. Perhaps the reason for this silence is that issues concerning the reliability of mini-CT-based T_0 values should be addressed through the ASTM balloting process for E1921, and that both CC-N-830-1 and CC-N-914 require the use of ASTM-valid T_0 values. A recent submittal to the NRC by the pressurized water reactor (PWR) Owners Group describes a planned project to collect an extensive database of T_0 values for PWR plants operating in the USA [58]. If executed, this project will include the testing of a substantial number of mini-CTs, the specimen being selected due to its frugal use of the limited archival and already irradiated materials that remain available. In their 15-page document requesting additional information [68] resulting from their review of [69], the NRC asked only one question about mini-CTs: *"discuss if additional uncertainty for mini-C(T) specimen data (i.e., uncertainly greater than what would be applied for larger C(T) specimens) would be included in the adjustment or margin terms."*

In summary, the application of mini-CT data in regulatory analysis remains a relatively new development, and this may explain the present lack of detailed questions from regulators about the mini-CT that extend beyond the much larger body of questions that regulators have asked about the MC over the past two to three decades.

5. Conclusions

The use of mini-CT specimens for master curve testing is a good option to reuse previously tested samples. It provides options for plants lacking sufficient amounts of material to continue to use conventional surveillance programs, during long-term operation. In particular, there is no bias in the reference temperature T_0 determined by testing mini-CTs when compared to larger specimens (see Figure 5). Nevertheless, certain aspects associated with mini-CT testing present unique challenges. In particular, the selection of appropriate test temperatures is crucial because the reduced measuring capacity of mini-CT specimens ($K_{Jclimit}$) limits the test temperature range over which censoring is unlikely. As a consequence, a higher number of tests ($N \approx 12$) is often required for the determination of a valid T_0 value using mini-CTs. This can be addressed in future revisions of the related standards [3,4]. In addition, even a modification of the 50 °C exclusion criterion could be considered by not invalidating data at very low test temperatures (i.e., $T < T_0 - 50$ °C).

Additional data and/or analyses will help to underpin the findings already discussed in this paper and lead to their resolution. Specific topics currently under consideration include the following:

- Censoring statistics (i.e., censoring probability as a function of test temperature)
- Re-evaluation of the censoring criterion for low upper shelf materials (cf. Equation (4)).
- Effects of side grooving and specific benefits.
- Effect of inhomogeneities and how they are handled in standards.

Author Contributions: Conceptualization, M.S. and S.C.; methodology, M.S. and S.C.; formal analysis, M.S., S.C., M.K., E.A., W.S. and M.Y.; investigation, M.S., S.C., M.K., E.A., W.S. and M.Y.; writing—original draft preparation, M.S., S.C., M.K., E.A., W.S. and M.Y.; writing—review and editing, M.S., S.C., M.K., E.A., W.S. and M.Y. All authors have read and agreed to the published version of the manuscript.

Funding: This project received funding from the Euratom Research & Training Programme 2019–2020 under grant agreement No. 900014 (FRACTESUS).

Data Availability Statement: Not applicable.

Conflicts of Interest: The authors declare no conflict of interest.

References

1. Wallin, K. Master curve analysis of the "Euro" fracture toughness dataset. *Eng. Fract. Mech.* **2002**, *69*, 451–481. [CrossRef]
2. Wallin, K. The scatter in KIC-results. *Eng. Fract. Mech.* **1984**, *19*, 1085–1093. [CrossRef]
3. *ASTM E1921*; Standard Test Method for Determination of Reference Temperature, T0, for Ferritic Steels in the Transition Range. ASTM International: West Conshohocken, PA, USA, 2021. [CrossRef]
4. *JEAC4216-2015*; Test Method for Determination of Reference Temperature T0 of Ferritic Steels. Japan Electric Association Code. Electric Association: Tokyo, Japan, 2015.
5. Brynk, T.; Uytdenhouwen, I.; Obermeier, F.; Altstadt, E.; Kopriva, R.; Serrano, M.; Arffman, P. Fractesus project: Final selection of RPV materials for unirradiated and irradiated round robins. *Am. Soc. Mech. Eng. Press. Vessel. Pip. Div. PVP* **2022**, *1*, 1–11. [CrossRef]
6. Cicero, S.; Lambrecht, M.; Swan, H.; Arffman, P.; Altstadt, E.; Petit, T.; Obermeier, F.; Arroyo, B.; Álvarez, J.A.; Lacalle, R. Fracture mechanics testing of irradiated RPV steels by means of sub-sized specimens: FRACTESUS project. *Procedia Struct. Integr.* **2020**, *28*, 61–66. [CrossRef]
7. Miura, N.; Soneda, N. Evaluation of Fracture Toughness by Master Curve Approach Using Miniature C(T) Specimens. In Proceedings of the ASME 2010 Pressure Vessels and Piping Division/K-PVP Conference, Bellevue, WA, USA, 18–22 July 2010; ASME: New York, NY, USA; Volume 1, pp. 593–602. [CrossRef]
8. Chaouadi, R.; Van Walle, E.; Scibetta, M.; Gérard, R. On the use of miniaturized ct specimens for fracture toughness characterization of RPV materials. *Am. Soc. Mech. Eng. Press Vessel Pip. Div. PVP* **2016**, *1B*, 1–10. [CrossRef]
9. Lambrecht, M.; Chaouadi, R.; Uytdenhouwen, I.; Gérard, R. Fracture toughness characterization in the transition and ductile regime of an a508 type weld metal with the mini-ct geometry before and after irradiation. *Am. Soc. Mech. Eng. Press. Vessel. Pip. Div. PVP* **2020**, *1*, 1–7. [CrossRef]
10. *ASTM E399*; Standard Test Method for Linear-Elastic Plane-Strain Fracture Toughness of Metallic Material. ASTM International: West Conshohocken, PA, USA, 2022; vol. 03.01. [CrossRef]
11. Scibetta, M.; Lucon, E.; Van Walle, E. Optimum use of broken Charpy specimens from surveillance programs for the application of the master curve approach. *Int. J. Fract.* **2002**, *116*, 231–244. [CrossRef]
12. Sokolov, M.A. Use of mini-CT specimens for fracture toughness characterization of low upper-shelf linde 80 weld. *Am. Soc. Mech. Eng. Press. Vessel. Pip. Div. PVP* **2017**, *1A*, 20–23. [CrossRef]
13. Yamamoto, M.; Kimura, A.; Onizawa, K.; Yoshimoto, K.; Ogawa, T.; Chiba, A.; Hirano, T.; Sugihara, T.; Sugiyama, M.; Miura, N. A round robin program of Master Curve evaluation using miniature C(T) specimens: First round robin test on uniform specimens of reactor pressure vessel material. *Am. Soc. Mech. Eng. Press. Vessel. Pip. Div. PVP* **2012**, *6*, 73–79. [CrossRef]
14. Yamamoto, M.; Kimura, A.; Onizawa, K.; Yoshimoto, K.; Ogawa, T.; Mabuchi, Y.; Viehrig, H.W.; Miura, N.; Soneda, N. A round Robin program of master curve evaluation using miniature C(T) specimens-3RD report: Comparison of T0 under various selections of temperature conditions. *Am. Soc. Mech. Eng. Press. Vessel. Pip. Div. PVP* **2014**, *1*, 1–7. [CrossRef]
15. Yamamoto, M.; Onizawa, K.; Yoshimoto, K.; Ogawa, T.; Mabuchi, Y.; Miura, N. Round Robin Program of Master Curve Evaluation Using Miniature C(T) Specimens—2nd Report: Fracture Toughness Comparison in Specified Loading Rate Condition. *Am. Soc. Mech. Eng. Press. Vessel. Pip. Div. PVP* **2013**, *1*, 1–8. [CrossRef]
16. Landes, J.D. J calculation from front face displacement measurement on a compact specimen. *Int. J. Fract.* **1980**, *16*, R183–R185. [CrossRef]
17. Miura, N.; Momoi, Y.; Yamamoto, M. Relation Between Front-Face and Load-Line Displacements on a C(T) Specimen by Elastic-Plastic Analysis. *Am. Soc. Mech. Eng. Press. Vessel. Pip. Div. PVP* **2015**, 1–6. [CrossRef]
18. Yamamoto, M.; Miura, N. Applicability of miniature C(T) specimens for the Master Curve evaluation of RPV weld metal. *Am. Soc. Mech. Eng. Press. Vessel. Pip. Div. PVP* **2015**, *1A*, 1–7. [CrossRef]
19. Wallin, K.; Yamamoto, M.; Ehrnstén, U. Location of Initiation Sites in Fracture Toughness Testing Specimens: The Effect of Size and Side Grooves. *Am. Soc. Mech. Eng. Press. Vessel. Pip. Div. PVP* **2016**, *1*, 1–9. [CrossRef]
20. Lambrecht, M.; Chaouadi, R.; Li, M.; Uytdenhouwen, I.; Scibetta, M. On the possible relaxation of the ASTM E1921 and ASTM E1820 Standard specifications with respect to the use of the mini-CT specimen. *Mater. Perform. Charact.* **2020**, *9*, 593–607. [CrossRef]
21. Lindqvist, S.; Kuutti, J. Sensitivity of the Master Curve reference temperature T0 to the crack front curvature. *Theor. Appl. Fract. Mech.* **2022**, *122*, 103558. [CrossRef]
22. Tobita, T.; Nishiyama, Y.; Ohtsu, T.; Udagawa, M.; Katsuyama, J.; Onizawa, K. Fracture Toughness Evaluation of Reactor Pressure Vessel Steels by Master Curve Method Using Miniature Compact Tension Specimens. *J. Press. Vessel Technol.* **2015**, *137*, 4–11. [CrossRef]
23. Sugihara, T.; Hirota, T.; Sakamoto, H.; Yoshimoto, K.; Tsutsumi, K.; Murakami, T. Applicability of miniature C(T) specimen to fracture toughness evaluation for the irradiated japanese reactor pressure vessel steel. *Am. Soc. Mech. Eng. Press. Vessel. Pip. Div. PVP* **2017**, *1*, 1–8. [CrossRef]
24. Sokolov, M.A.; Nanstad, R.K. Comparison of irradiation-induced shifts of KJc and Charpy impact toughness for reactor pressure vessel steels. *ASTM Spec. Tech. Publ.* **1999**, *1325*, 167–190.
25. Sokolov, M.A. Use of mini-CT specimens for fracture toughness characterization of low upper-shelf linde 80 weld before and after irradiation1. *Am. Soc. Mech. Eng. Press. Vessel. Pip. Div. PVP* **2018**, *1*, 1–6. [CrossRef]

26. Server, W.; Sokolov, M.; Yamamoto, M.; Carter, R. Inter-Laboratory Results and Analyses of Mini-C(T) Specimen Testing of an Irradiated Linde 80 Weld Metal. *Am. Soc. Mech. Eng. Press. Vessel. Pip. Div. PVP* **2018**, *1*, 1–5. [CrossRef]
27. Yamamoto, M. Trial study of the master curve fracture toughness evaluation by mini-C(T) specimens for low upper shelf weld metal linde-80. *Am. Soc. Mech. Eng. Press. Vessel. Pip. Div. PVP* **2018**, *1*, 1–8. [CrossRef]
28. Yamamoto, M.; Kirk, M.; Shinko, T. Master curve evaluation using the fracture toughness data at low test temperature of T-T0<-50 °C. *Am. Soc. Mech. Eng. Press. Vessel. Pip. Div. PVP* **2022**, *1*, 1–8. [CrossRef]
29. Yamamoto, M.; Miura, N. Applicability of miniature-c(T) specimen for the master curve evaluation of rpv weld metal and heat affected zone. *Am. Soc. Mech. Eng. Press. Vessel. Pip. Div. PVP* **2016**, *1*, 1–8. [CrossRef]
30. Ha, Y.; Tobita, T.; Takamizawa, H.; Nishiyama, Y. Fracture toughness evaluation of neutron-irradiated reactor pressure vessel steel using miniature-C(T) specimens. *Am. Soc. Mech. Eng. Press. Vessel. Pip. Div. PVP* **2017**, *1*, 1–5. [CrossRef]
31. Yamamoto, M. The Master Curve Fracture Toughness Evaluation of Irradiated Plate Material JRQ Using Miniature-C(T) Specimens. *Am. Soc. Mech. Eng. Press. Vessel. Pip. Div. PVP.* **2017**, *1*, 1–8. [CrossRef]
32. Yamamoto, M.; Kobayashi, T. Evaluation of Through Wall Fracture Toughness Distribution of IAEA Reference Material JRQ by Mini-C(T) Specimens and the Master Curve Method. *Am. Soc. Mech. Eng. Press. Vessel. Pip. Div. PVP.* **2018**, *1*, 1–8. [CrossRef]
33. Uytdenhouwen, I.; Chaouadi, R. Effect of neutron irradiation on the mechanical properties of an a508 cl.2 forging irradiated in a bami capsule. *Am. Soc. Mech. Eng. Press. Vessel. Pip. Div. PVP.* **2020**, *1*, 2–10. [CrossRef]
34. Chen, X.F.; Sokolov, M.A.; Gonzalez De Vicente, S.M.; Katoh, Y. Specimen Size and Geometry Effects on the Master Curve Fracture Toughness Measurements of EUROFER97 and F82H Steels. *Am. Soc. Mech. Eng. Press. Vessel. Pip. Div. PVP.* **2022**, *1*, 1–9. [CrossRef]
35. Ha, Y.; Tobita, T.; Ohtsu, T.; Takamizawa, H.; Nishiyama, Y. Applicability of Miniature Compact Tension Specimens for Fracture Toughness Evaluation of Highly Neutron Irradiated Reactor Pressure Vessel Steels. *J. Press. Vessel Technol.* **2018**, *140*, 1–6. [CrossRef]
36. Yamamoto, M.; Sakuraya, S.; Kitsunai, Y.; Kirk, M. Practical procedure of test temperature selection for mini-C(T) master curve evaluation. *Am. Soc. Mech. Eng. Press. Vessel. Pip. Div. PVP* **2022**, *1*, 1–7. [CrossRef]
37. Takamizawa, H.; Tobita, T.; Ohtsu, T.; Katsuyama, J.; Nishiyama, Y.; Onizawa, K. Finite element analysis on the application of MINI-C(T) test specimens for fracture toughness evaluation. *Am. Soc. Mech. Eng. Press. Vessel. Pip. Div. PVP* **2015**, *1A*, 1–7. [CrossRef]
38. Sánchez, M.; Cicero, S.; Arroyo, B.; Cimentada, A. On the Use of Mini-CT Specimens to Define the Master Curve of Unirradiated Reactor Pressure Vessel Steels with Relatively High Reference Temperatures. *Theoretical and Applied Fracture Mechanics* **2023**, *124*, 103736. [CrossRef]
39. Hall, J.B.; Yoon, K.K. Quasi-Static Loading Rate Effect on the Master Curve Reference Temperature of Ferritic Steels and Implications. *Am. Soc. Mech. Eng. Press. Vessel. Pip. Div. PVP* **2003**, *1*, 9–14. [CrossRef]
40. Yamamoto, M.; Carter, R.; Viehrig, H.; Lambrecht, M. A Round Robin Program of Master Curve Evaluation using Miniature C (T) Specimens (Comparison of T0 for a Weld Metal). 20–25 August 2017.
41. International Atomic Energy Agency (IAEA). *Application of Surveillance Programme Results to Reactor Pressure Vessel Integrity Assessment. Results of a Coordinated Research Project 2000–2004*; International Atomic Energy Agency (IAEA): Vienna, Austria, 2005; Volume 1556.
42. Ickes, M.R.; Brian Hall, J.; Carter, R.G. Fracture toughness characterization of low upper-shelf linde 80 weld using mini-C(T) specimens. *Am. Soc. Mech. Eng. Press. Vessel. Pip. Div. PVP* **2018**, *1*, 1–6. [CrossRef]
43. McCabe, D.; Nanstad, R.; Iskander, S.; Heatherly, D.; Swain, R. NUREG/CR-5736; *Evaluation of WF-70 Weld Metal from the Midland Unit 1 Reactor Vessel*; U.S. Nuclear Regulatory Commission: Rockville, MD, USA, 2000.
44. Han, W.; Yabuuchi, K.; Kasada, R.; Kimura, A.; Wakai, E.; Tanigawa, H.; Liu, P.; Yi, X.; Wan, F. Application of small specimen test technique to evaluate fracture toughness of reduced activation ferritic/martensitic steel. *Fusion Eng. Des.* **2017**, *125*, 326–329. [CrossRef]
45. Sokolov, M.A. Use of mini-CT specimens for fracture toughness characterization of irradiated highly embrittled weld. *Am. Soc. Mech. Eng. Press. Vessel. Pip. Div. PVP* **2022**, *1*, 10–13. [CrossRef]
46. Zhou, Z.; Tong, Z.; Qian, G.; Berto, F. Specimen Size Effect on the Ductile-Brittle Transition Reference Temperature of A508-3 Steel. *Theoretical and Applied Fracture Mechanics* **2019**, *104*, 102370. [CrossRef]
47. Wallin, K.; Saario, T.; Törrönen, K. Statistical Model for Carbide Induced Brittle Fracture in Steel. *Met. Sci.* **1984**, *18*, 13–16. [CrossRef]
48. Wallin, K. Irradiation Damage Effects on the Fracture Toughness Transition Curve Shape for Reactor Vessel Steels. *Int. J. Pres. Vessel. Pip.* **1993**, *55*, 61–79. [CrossRef]
49. ASME Boiler and Pressure Vessel Code Case N-629. *Use of Fracture Toughness Test Data to Establish Reference Temperature for Pressure Retaining Materials*; Section XI, Division 1; ASME: New York, NY, USA, 1999.
50. ASME Boiler and Pressure Vessel Code Case N-631. *Use of Fracture Toughness Test Data to Establish Reference Temperature for Pressure Retaining Materials Other Than Bolting for Class 1 Vessels Section III, Division 1*; ASME: New York, NY, USA, 1999.
51. Electric Power Research Institute. *Application of Master Curve Fracture Toughness Methodology for Ferritic Steels (PWRMRP-01): PWR Materials Reliability Project (PWRMRP)*; EPRI: Palo Alto, CA, USA, 1999; TR-108390 Revision 1.

52. Yoon, K.K. *Fracture Toughness Characterization of WF-70 Weld Metal*; Report to the B&W Owners Group Materials Committee, BAW-2202; Babcock and Wilcox Company: Nuclear Power Division, Virginia, September 1993.
53. Lott, R.G.; Kirk, M.T.; Kim, C.C. Master Curve Strategies for RPV Assessment. Westinghouse Electric Company: Pittsburgh, PA, USA, WCAP-15075. September 1998; Available on the USNRC website at Legacy ADAMS 9811240260 and at ADAMS ML111861647.
54. NRC Safety Evaluation Report on Kewaunee Master Curve Submittal, Letter of 1st May 2001 from Lamb to Reddemann, ADAMS ML011210180.
55. Lee, B.S.; Hong, J.H.; Lee, D.H.; Choi, D.G. RTPTS Re–Evaluation of Kori–1 Rpv Beltline Weld By Master Curve Tests. In Proceedings of the Second International Symposium on Nuclear Power Plant Life Management, Shanghai, China, 15–18 October 2007. Paper Number IAEA-CN-155-063.
56. Framatome ANP, Inc. Initial RT_{NDT} of Linde-80 Weld Materials. Report to the PWR Owners Group, BAW-2308 Rev. 2A. March 2008.
57. Mayfield, M.; Vassilaros, M.; Hackett, E.; Wichman, K.; Strosnider, J.; Shao, L. Application of revised fracture toughness curves in pressure vessel integrity analysis. In Proceedings of the Transactions of the 14th International Conference on Structural Mechanics in Reactor Technology (SMiRT 14), Lyon, France, 12–22 August 1997. G01/2.
58. Kirk, M.; Hashimoto, Y.; Nomoto, A. Application of a Machine Learning Approach Based on Nearest Neighbors to Extract Embrittlement Trends from RPV Surveillance Data. *J. Nucl. Mater.* **2022**, *568*, 153886. [CrossRef]
59. Bamford, W.; Stevens, G.; Griesbach, T.; Malik, S. *The 2000 Technical Basis for Revised P-T Limit Curve Methodology*; ASME Pressure Vessel and Piping Meeting: Seattle, WA, USA, 2000.
60. Electric Power Research Institute. *Methods to Address the Effects of Irradiation Embrittlement in Section XI of the ASME Code: Estimation of an Irradiated Reference Temperature Using either Traditional Charpy Approaches or Master Curve Data*; EPRI: Palo Alto, CA, USA, 2021; p. 3002020911.
61. Kirk, M. *The Technical Basis for Application of the Master Curve to the Assessment of Nuclear Reactor Pressure Vessel Integrity*; ADAMS ML093540004; USA Nuclear Regulatory Commission: Washington, DC, USA, October 2002.
62. Sokolov, M.; Nanstad, R.; Remec, I.; Baldwin, C.; Swain, R. *Fracture Toughness of an Irradiated, Highly Embrittled Reactor Pressure Vessel Weld*; Oak Ridge National Laboratory: Oak Ridge, TN, USA, 2003; ORNL/TM-2002/293.
63. Wallin, K. The Elusive Temperature Dependence of the Master Curve. In Proceedings of the 13th International Conference on Fracture 2013, ICF-13, Beijing, China, 16–21 June 2013; 2013; Volume 7, pp. 5609–5617.
64. *KTA-3203*; Surveillance of the Irradiation Behavior of Reactor Pressure Vessel Materials of LWR Facilities. Safety Standards of the Nuclear Safety Standards Commission (KTA): Salzgitter, Germany, 2011.
65. *ENSI-B01/d*; Alterungsüberwachung, Richtlinie für die Schweizerischen Kernanlagen. Swiss Federal Nuclear Safety Inspectorate ENSI: Brugg, Switzerland, 2012.
66. *JEAC 4206-2016*; Method of Verification Tests of the Fracture Toughness for Nuclear Power Plant Components. Japan Electric Association Code. Electric Association: Tokyo, Japan, 2016.
67. Electric Power Research Institute. *Technical Basis for ASME Code Case N-830-1, Revision 1 (MRP-418, Revision 1): Direct Use of Master Curve Fracture Toughness Curve for Pressure-Retaining Materials of Class 1 Vessels, Section XI*; EPRI: Palo Alto, CA, USA, 2019; p. 3002016008.
68. U.S. Nuclear Regulatory Commission's request for additional information by the office of nuclear reactor regulation on topical report PWROG-18068-NP, revision 1. Use of Direct Fracture Toughness for Evaluation of RPV Integrity for the Pressurized Water Reactor Owners Group Project No. 99902037; EPID: L-2021-TOP-0027, ADAMS ML2208A246. USA Nuclear Regulatory Commission: Washington, DC, USA, 2021.
69. Hall, J.B. *Use of Direct Fracture Toughness for Evaluation of RPV Integrity*; PWROG-18068-Np-Rev. 1; Westinghouse Electric Company: Pittsburgh, PA, USA, July 2021.